

## Superradiant emission from Bloch oscillations in semiconductor superlattices

R. Martini,\* G. Klose, H. G. Roskos,<sup>†</sup> and H. Kurz

Institut für Halbleitertechnik II, Rheinisch-Westfälische Technische Hochschule (RWTH) Aachen, Sommerfeldstrasse 24, D-52056 Aachen, Germany

H. T. Grahn and R. Hey

Paul Drude Institut für Festkörperelektronik, Hausvogteiplatz 5-7, D-10117 Berlin, Germany

(Received 22 May 1996)

The superradiant character of submillimeter-wave emission from optically excited electronic Bloch oscillations in a GaAs/Al<sub>x</sub>Ga<sub>1-x</sub>As superlattice is investigated by time-resolved terahertz emission spectroscopy. The intensity of the radiation and its decay time are studied as a function of the density of excited charge carriers. From the measured emission efficiency, the spatial amplitude of the charge oscillations is estimated. [S0163-1829(96)52144-2]

Bloch oscillations of electrons in semiconductor superlattices, excited impulsively by subpicosecond laser pulses, are attractive as a source of coherent terahertz (THz) electromagnetic pulses because the frequency of the radiation can be tuned from 0.2 to 10 THz by an electric dc bias field.<sup>1-6</sup> Until now, only fundamental aspects of THz emission at low optical excitation power and thus at a low density of the photoexcited charge carriers of about  $1-3 \times 10^9 \text{ cm}^{-2}$  per well (corresponding volume density:  $1-3 \times 10^{15} \text{ cm}^{-3}$ ) have been investigated.<sup>4</sup> So far, the time-averaged power of the THz pulses has not exceeded 0.1 nW.<sup>7</sup> To be of practical interest, the power of the radiation must be increased by orders of magnitude. A straightforward way to enhance the THz output power should be the increase of the optical excitation power. As the photoexcited Bloch oscillations are coherent charge oscillations they are expected to emit radiation in a superradiant manner (for a discussion see Ref. 7). Simple calculations with superradiance theory neglecting both many-particle effects and reabsorption of the THz radiation predict a quadratic scaling of the THz pulse energy with the excitation density.<sup>7,8</sup> This dependence, however, is only expected if the coherence of the polarization associated with the wave-packet oscillations does not degrade with increasing excitation density. Up to now, the influence of the excitation density on the dephasing of Bloch oscillations is unknown. To date, neither THz-emission experiments probing the electron occupation density (*intraband* polarization Refs. 9 and 10) nor four-wave-mixing (FWM) measurements of the nonlinear third-order interband polarization have been carried out as a function of density.

In this paper, we investigate experimentally the excitation-density dependence of both the power and the decay time constant of THz radiation from Bloch oscillations in a GaAs/Al<sub>x</sub>Ga<sub>1-x</sub>As superlattice. The measurements are performed with a *pin*-sample design to avoid severe quasistatic field-screening effects by accumulated charge carriers that have prevented such measurements in our previous Schottky-type samples.<sup>1-6</sup> The band-structure diagram of the *pin* sample without external bias is displayed in the inset of Fig. 1. The undoped superlattice consists of 35 periods of 9.7-nm-wide GaAs wells and 1.7-nm-wide Al<sub>0.3</sub>Ga<sub>0.7</sub>As

barriers. The first and the last Al<sub>0.3</sub>Ga<sub>0.7</sub>As barrier of the superlattice are separated from the surrounding doped regions by 25 nm of nominally undoped GaAs. A 570-nm-thick graded Al<sub>x</sub>Ga<sub>1-x</sub>As stop-etch layer with a maximum Al content of  $x = 0.5$  provides electric contact to the substrate ( $n^+$ -doping:  $2 \times 10^{18} \text{ Si atoms/cm}^3$ ). A 30-nm-thick  $p^+$ -doped GaAs layer serves as the top contact of the structure. The choice of this extraordinarily thin cover layer limits absorption losses of the THz radiation passing through it. A high doping concentration ( $3 \times 10^{19} \text{ C atoms/cm}^3$ ) ensures good Ohmic contacts without annealing, and an abrupt field onset in the intrinsic region of the diode. The samples are patterned into mesa structures with a diameter of 450  $\mu\text{m}$  to

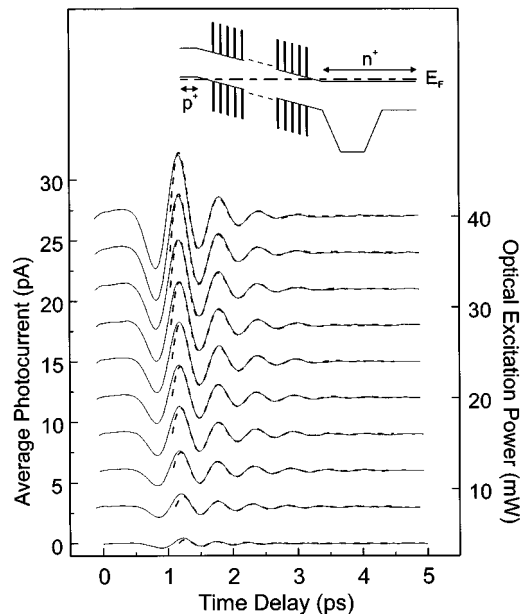


FIG. 1. Detected THz transients for various optical excitation powers. The dashed lines are fits with the function given in the text. The inset illustrates the band structure of the unbiased *pin* superlattice structure (bandgap not drawn to scale). The substrate is to the right side.

limit the current. Ohmic Cr/Au ring contacts leave an inner 390- $\mu\text{m}$ -wide window region unmetallized and thus transparent for optical and THz radiation.

The experiments are performed in a standard THz-emission-spectroscopy setup.<sup>1,2</sup> The sample is mounted in a closed-cycle cryostat and held at a temperature of 20 K. Bloch oscillations are excited by 150-fs pulses from a Kerr-lens mode-locked Ti:sapphire laser (repetition time  $\tau_{\text{Rep}} = 13$  ns) operating at photon energies centered below (1.542 eV) or above (1.557 eV) band edge to excite mainly excitons or continuum states. The optical beam hits the sample at an angle of 45°. Coherent THz pulses emitted in the direction of the reflected optical beam are detected as a function of time with a photoconductive antenna made from low-temperature-grown GaAs.

Figure 1 displays the detected Bloch transients in dependence of the average optical excitation power. The amplitude of the detected electric field is given in terms of the measured photocurrent through the antenna. The photon energy of the excitation pulses is 1.557 eV, the bias voltage 1.175 V. With increasing excitation density, the amplitude of the radiation rises while the signal decay becomes faster. From the lowest to the highest excitation power, the frequency of the Bloch oscillations changes from 2.1 THz to 1.7 THz. The frequency shift indicates residual screening effects, but compared to the previous Schottky-type samples, this 20% shift for a variation of the excitation power over one order of magnitude represents a drastic improvement by the *pin* design.

Frequency  $\omega$ , amplitude  $A$ , and decay time  $\tau$  of the THz transients in Fig. 1 are extracted by fitting the data with the function  $A \exp[-(t-t_0)/\tau] \cos[\omega \cdot (t-t_0)]$  for  $t > t_0$ . This temporal dependence is expected from one-dimensional semiclassical calculations for the radiation from Bloch oscillations upon excitation with a  $\delta$  pulse at  $t = t_0$ . Due to the finite pulse length of the exciting pulse and the limited bandwidth of the antenna response function deviations from the model wave form occur around and before  $t_0$ . Therefore only the data after  $t \geq 1.5$  ps are taken into account for the fit procedure in order to suppress contributions from these deviations and from unexpected instantaneous polarization.<sup>11</sup> The unknown value of  $t_0$  is the extrapolated peak position of the fit function close to the first maximum of the THz transients. The fitted curves (see dashed lines in Fig. 1) fully reproduce the experimental transients *including* the region right after the first maxima of the fit ( $t_0$ ).

The amplitude  $A$  of the fit to the Bloch transients is displayed in Fig. 2 as a function of the density  $n_{\text{exc}}$  of the photogenerated charge carriers.  $n_{\text{exc}}$  is estimated from the excitation power by taking reflection losses and an estimated absorption of 60% of the light in the sample into account.  $A$  is corrected for the frequency shift that produces an amplitude change because of the spectral characteristics of the receiver antenna. The peak amplitude of the THz transients (circles in Fig. 2) rises linearly with the carrier density as expected from simple superradiance theory. The linearity is maintained up to the highest carrier density of  $2.2 \times 10^{10} \text{ cm}^{-2}$  per well. This density is still below the Mott density marking the disappearance of the exciton resonances. Figure 2 displays also the peak amplitude of the Bloch transients for an excitation photon energy of 1.542 eV

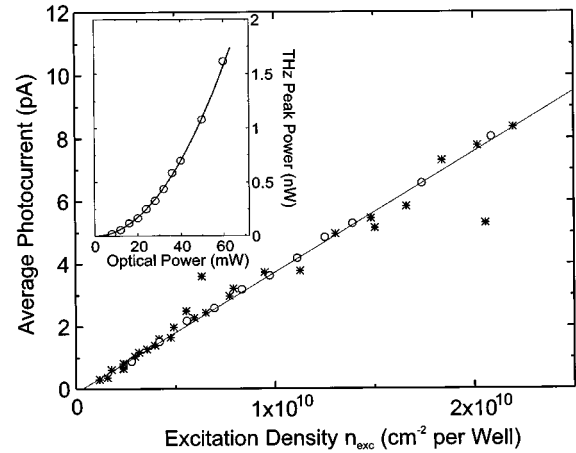


FIG. 2. Amplitude of the THz radiation as a function of the density of the photoexcited carriers. Data for two excitation photon energies are shown: 1.542 eV (stars) and 1.557 eV (circles). The inset shows the calculated THz peak power as a function of the optical power for the excitation energy of 1.557 eV. The 1.542-eV data scatter more strongly because of a lower signal-to-noise ratio in the particular measurements. The full lines are guides to the eye.

(stars). Here,  $n_{\text{exc}}$  is estimated from the excitation power by assuming an absorption coefficient of 30%. Comparing the two data sets (circles and stars) of Fig. 2, no significant difference is found. Obviously, the peak amplitude (absolute value and density dependence) is comparable for the two excitation conditions within the experimental uncertainties. This is an indication that the intraband polarization as probed by THz emission spectroscopy is similar in strength for these two cases, quite in contrast to FWM measurements on bulk GaAs that are dominated by exciton transitions.<sup>12</sup>

A rough estimate of the power of the incident THz radiation can be obtained from the measured antenna photocurrent if the sensitivity of the detection setup has been quantified with a surface emitter, calibrated according to Ref. 13. The inset of Fig. 2 displays the time-averaged peak power of the THz radiation, determined from the values of  $A$  with this procedure, as a function of the optical input power. At the highest input power of 60 mW, the time-averaged peak power of the THz pulses is about 1.75 nW (external conversion efficiency:  $3 \times 10^{-8}$ ). This is an improvement by a factor of 20 over the previously reported values.<sup>7</sup>

For practical purposes, the time-averaged power of the THz radiation  $\langle P \rangle$  (i.e., the pulse energy times  $\tau_{\text{Rep}}^{-1}$ ) is a more significant quantity than the time-averaged peak power considered above. In contrast to the latter,  $\langle P \rangle$  depends strongly on the decay time  $\tau$  of the THz transients. As  $\tau$  decreases when the excitation density is raised,  $\langle P \rangle$  does not scale quadratically with the input power.

Figure 3 displays the fit values of  $\tau$  (inset) and the corresponding homogeneous linewidth  $\Gamma = 2\hbar/\tau$  (main part of the figure) as a function of  $n_{\text{exc}}$  for excitation photon energies of 1.557 eV (circles) and 1.542 eV (stars). For both photon energies,  $\tau$  decreases continuously from 1 ps at the lowest densities of  $1.5 \times 10^9$  carriers per  $\text{cm}^2$  per well to below 0.4 ps at  $2.2 \times 10^{10}$  carriers per  $\text{cm}^2$  per well. We observe no significant difference between the predominant excitation of

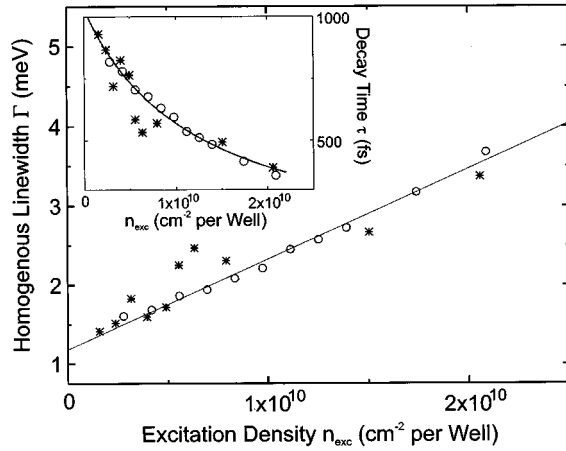


FIG. 3. Homogeneous linewidth  $\Gamma$  and decay time constant (inset) of the THz pulses as a function of excitation density. The full lines are fits with the function discussed in the text.

exciton transitions versus one of continuum states.

In order to analyze the excitation-density dependence of  $\Gamma$  quantitatively, we fit the data with the function

$$\Gamma(n_{\text{exc}}) = \Gamma(0) + \vartheta n_{\text{exc}}, \quad (1)$$

successfully employed before to model the signal decay in FWM measurements on excitons.<sup>14,15</sup>  $\Gamma(0)$  stands for density-independent dephasing due to interface-roughness and alloy scattering as well as inhomogeneous broadening, whereas the density-dependent part of Eq. (1) represents carrier-carrier scattering. Our data are well described by a fit curve (full line) with the following values:  $\vartheta = 9 \times 10^{-11}$  meV  $\times$  cm<sup>2</sup>  $\times$  well and  $\Gamma(0) = 1.2$  meV. With these values, one estimates that carrier-carrier scattering dominates the signal decay in our experiments for  $n_{\text{exc}} > 1.3 \times 10^{10}$  carriers per cm<sup>2</sup> per well. We observe no significant difference between the data for predominant excitation of excitons or free carriers in our experiments. In contrast to the dephasing of the interband polarization in FWM experiments<sup>6</sup> the dephasing of the intraband polarization probed by THz emission depends little on the character of the excited transitions.

Finally, we estimate the spatial amplitude of the Bloch oscillations from the peak power of the THz pulses. For that purpose the peak power of the THz radiation *inside* the superlattice region is needed. Calculating THz beam transmission through the highly doped top contact layer (taking multiple reflections within this layer into account) one estimates that only 5% of the power incident from the superlattice is transmitted through the contact, 37% is lost by Drude absorption, 58% by reflection into the substrate where it is absorbed (reabsorption in the superlattice region is negligible for the carrier densities of the experiments). The peak power  $P_0 = P(t=0)$  is estimated from the experimentally determined time-averaged power by correcting for the transmission coefficient and the assumed THz pulse duration of 1 ps.

The theory of superradiance derives  $P_0$  for our experimental conditions as

$$P_0 = \frac{e^2}{4c\epsilon_0 n'} Z_{\text{Bloch}}^2 \omega^2 n_{\text{exc}}^2 W^2 F \frac{\sin^2(\alpha)}{\cos(\alpha)}. \quad (2)$$

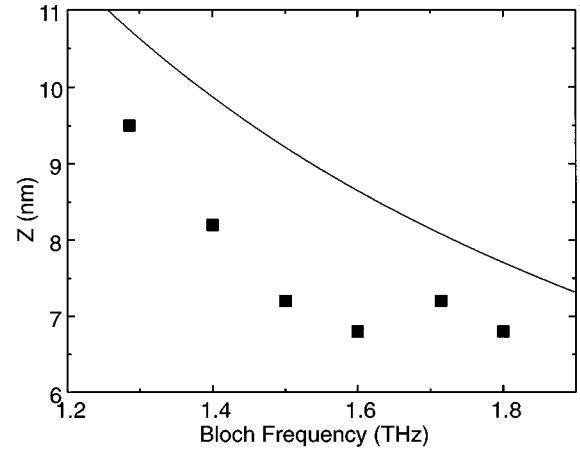


FIG. 4. Frequency dependence of the electron-hole separation matrix element  $Z_{\text{Bloch}}$ . Full squares: experimental data, full line: quantum-mechanical model neglecting Coulomb interaction.

Equation (2) extends Eq. (19) of Ref. 7 by taking the refractive index  $n'$  of the semiconductor into account.  $W$  is the number of periods in the superlattice,  $F$  the excited area, and  $\alpha$  the propagation angle of the THz radiation within the superlattice relative to the growth direction.  $Z_{\text{Bloch}}$  denotes the electron-hole separation matrix element corresponding to the spatial amplitude of the Bloch oscillations in the particle picture. Equation (2) enables us to estimate  $Z_{\text{Bloch}}$  from the experimentally determined peak power within a factor of 2.

Figure 4 displays  $Z_{\text{Bloch}}$  for various Bloch frequencies (measurements at various bias voltages) averaged over the range of excitation densities covered in Figs. 2 and 3.  $Z_{\text{Bloch}}$  is found to be inversely proportional to frequency, decreasing from 9.5 nm at 1.3 THz to 6.8 nm at 1.8 THz. Hence, the full amplitude  $2Z_{\text{Bloch}}$  of the oscillations is between one and two spatial periods of the superlattice in this frequency region. The semiclassical theory of Bloch oscillations predicts an amplitude of  $Z_{\text{SC}} = 0.5 \Delta E d / (\hbar \omega)$ , with  $\Delta E$  being the width of the electronic miniband. This relation implies that the maximum velocity  $v$  of the wave packet,  $v \propto Z_{\text{SC}} \omega$ , is independent of the bias field. The semiclassical model predicts the  $1/\omega$  dependence of  $Z_{\text{Bloch}}$ , but the absolute values calculated with the miniband width  $\Delta E = 18$  meV of our sample are by a factor of 2 larger ( $Z_{\text{SC}} = 19$  nm at 1.3 THz, and 14 nm at 1.8 THz) than the values derived from the experiment. Better agreement is achieved with a quantum-mechanical model<sup>3</sup> (full line in Fig. 4). The remaining discrepancy is likely to have two origins: (i) the peak power determination has a considerable experimental uncertainty; (ii) both models neglect Coulomb attraction between electrons and holes, that tends to reduce  $Z_{\text{Bloch}}$ .

In conclusion, we have investigated the strength of coherent THz emission from optically excited Bloch oscillations as a function of excitation density. The superradiant character of the emission is proven up to excitation densities of  $2.2 \times 10^{10}$  carriers per cm<sup>2</sup> per well. The highest peak powers of the THz radiation exceed the values reported previously by a factor of 20. An external power conversion efficiency (measured THz peak power versus absorbed optical power) of  $3 \times 10^{-8}$  is reached. Further enhancement of the emission efficiency suffers from the faster decay of the THz

transients at higher excitation density resulting from stronger carrier-carrier scattering. It is remarkable, however, that the decay is unaffected when predominantly uncorrelated electron-hole pairs are excited instead of excitons. This is in pronounced contrast to the interband dynamics. Further efficiency enhancement by more than one order of magnitude without faster signal decay should be achievable by better output coupling (now only 5%) and excitation and emission at more oblique angles. From the measured peak

power of the THz radiation, the spatial amplitude of the Bloch oscillations is estimated. It is found to depend inversely on the Bloch frequency as expected from semiclassical theory.

We acknowledge stimulating discussions with F. Wolter and P. Haring Bolivar. This project has been supported by BMBF under Contract No. 13N6526 and by DFG under Contract No. RO 770/4-2.

\*Electronic address: martini2@basl.rwth-aachen.de

†Electronic address: roskos@basl.rwth-aachen.de

<sup>1</sup>C. Waschke, H. G. Roskos, R. Schwedler, K. Leo, H. Kurz, and K. Köhler, Phys. Rev. Lett. **70**, 3319 (1993).

<sup>2</sup>H. G. Roskos, in *Festkörperprobleme/Advances in Solid State Physics*, edited by R. Helbig (Vieweg, Braunschweig, Germany, 1994), Vol. 34, pp. 297–315.

<sup>3</sup>P. Leisching, P. Haring Bolivar, W. Beck, Y. Dhaibi, F. Brüggemann, R. Schwedler, H. Kurz, K. Leo, and K. Köhler, Phys. Rev. B **50**, 14 389 (1994).

<sup>4</sup>C. Waschke, P. Leisching, P. Haring Bolivar, R. Schwedler, F. Brüggemann, H. G. Roskos, K. Leo, H. Kurz, and K. Köhler, Solid State Electron. **37**, 1321 (1994).

<sup>5</sup>H. G. Roskos, C. Waschke, R. Schwedler, P. Leisching, Y. Dhaibi, H. Kurz, and K. Köhler, Superlattices Microstruct. **15**, 281 (1994).

<sup>6</sup>P. Leisching, T. Dekorsy, H. J. Bakker, K. Köhler, and H. Kurz, Phys. Rev. B **52**, 18 015 (1995).

<sup>7</sup>K. Victor, H. G. Roskos, and C. Waschke, J. Opt. Soc. Am. B **11**, 2470 (1994).

<sup>8</sup>R. H. Dicke, Phys. Rev. **93**, 99 (1953).

<sup>9</sup>M. Axt, G. Bartels, and A. Stahl, Phys. Rev. Lett. **76**, 2543 (1996).

<sup>10</sup>T. Meier, F. Rossi, P. Thomas, and S. W. Koch, Phys. Rev. Lett. **75**, 2558 (1995).

<sup>11</sup>S. L. Chuang, S. Schmitt-Rink, B. I. Greene, P. N. Saeta, and A. F. J. Levi, Phys. Rev. Lett. **68**, 102 (1992).

<sup>12</sup>A. Lohner, L. Rick, P. Leisching, A. Leitenstorfer, T. Elsaesser, T. Kuhn, F. Rossi, W. Stolz, Phys. Rev. Lett. **71**, 77 (1993).

<sup>13</sup>M. van Exter and D. R. Grischkowsky, IEEE Trans. Microwave Theory Tech. **MTT-38**, 1684 (1990).

<sup>14</sup>L. Schultheiss, J. Kuhl, A. Honold, and C. W. Tu, Phys. Rev. Lett. **57**, 1635 (1986).

<sup>15</sup>J. Kuhl, A. Honold, L. Schultheis, and C. W. Tu, in *Festkörperprobleme/Advances in Solid State Physics*, edited by R. Helbig (Vieweg, Braunschweig, Germany, 1989), Vol. 29, pp. 157–181.